metals

MDPI

Article

Effect on Microstructure and Performance of B_4C Content in B_4C/Cu Composite

Dayu Shu [1], Xiuqing Li [2,*] and Qingxia Yang [3]

[1] Southwest Technology and Engineering Research Institute, Chongqing 400039, China; shudayu1980@163.com
[2] National Joint Engineering Research Center for Abrasion Control and Molding of Metal Materials, Henan University of Science & Technology, Luoyang 471003, China
[3] School of Vehicle and Traffic Engineering, Henan University of Science & Technology, Luoyang 471003, China; 9905679@haust.edu.cn
* Correspondence: xqli@haust.edu.cn; Tel.: +86-0379-6427-0020

Abstract: In this paper, boron carbide (B_4C) ceramics were added to a copper (Cu) base, to improve the mechanical properties and wear resistance of pure copper. The B_4C/Cu composites with different B_4C contents, were obtained by mechanical mixing and discharge plasma sintering methods. Scanning electron microscopy (SEM), energy spectrum analysis (EDS), and electron probe microanalysis (EPMA) were used, to observe and analyze the microstructures of the B_4C/Cu composites. The influences of the B_4C content on the hardness, density, conductivity, and wear resistance were also studied. The experimental results show that B_4C has an important effect on Cu. With increasing B_4C content, both the density and conductivity of the B_4C/Cu composites gradually decrease. The hardness of the Cu-15 wt.% B_4C composite has the highest value, 86 HBW (Brinell hardness tungsten carbide ball indenter), which is 79.2% higher than that of pure copper. However, when the B_4C amount increases to 20 wt.%, the hardness decreases due to the metallic connection being weakened in the material. The Cu-15 wt.% B_4C composite has the lowest volume loss, indicating that it has the best wear resistance. Analyses of worn B_4C/Cu composite surfaces suggest that deep and narrow grooves, as well as sharp ridges, appear on the worn pure Cu surface, but on the worn Cu-15 wt.% B_4C composite surface, the furrows become shallow and few. In particular, ridge formation cannot be found on the worn Cu-15 wt.% B_4C composite surface, which represents the enhancement in wear resistance.

Keywords: Cu; boron carbide; properties; wear resistance

Citation: Shu, D.; Li, X.; Yang, Q. Effect on Microstructure and Performance of B_4C Content in B_4C/Cu Composite. *Metals* **2021**, *11*, 1250. https://doi.org/10.3390/met11081250

Academic Editor: Andreas Chrysanthou

Received: 13 July 2021
Accepted: 4 August 2021
Published: 6 August 2021

1. Introduction

Metallic copper (Cu) is widely applied in the fields of electrical, transportation, construction, and aerospace, similarly to electric cable, heating, connector, lead frame, radiator, commutator, and brake facing, because of its excellent conductivity and thermal conductivity and the low price of raw materials. However, the hardness, strength and wear resistance of Cu are low, and cannot meet the increasing requirements of modern science and technology on material properties. To overcome the low hardness and low wear resistance of pure Cu, Cu-based composites have been widely studied [1–4]. For example, Shaik et al. [1] studied the mechanical properties and tribological characteristics of Cu–zirconium diboride (ZrB_2) composites against silicon carbide (SiC) emery paper. The results suggested that, when the ZrB_2 content was 10 wt.%, the Cu–ZrB_2 composites possessed the maximum hardness and the maximum yield strength, and the steady-state friction coefficient of Cu decreased, from 0.56 to 0.16, when ZrB_2 was added. In particular, the wear coefficient of the Cu-3 wt.% ZrB_2 composites drastically decreased by 7.33 times. Guiderdoni et al. [2] researched the effect of double-walled carbon nanotubes on the hardness and friction performance of Cu matrix composites. The results showed that, compared to pure copper, the

Vickers microhardness was doubled when double-walled carbon nanotubes were added, and the wear was very low.

The hardness of boron carbide (B_4C) ceramics ranks third among known materials in the world, with the advantages of low density, high oxidation resistance, high acid and alkali corrosion resistance, high wear resistance, etc. In addition, it has stable high-temperature strength and can absorb neutrons [5–9]. B_4C has been added to the matrix of many metal materials, as a strengthening phase to improve their performance [10–16]. For example, Lyu et al. [10] added B_4C particles into a Q235 steel substrate and found that the wear resistance could be greatly improved. In addition, Yahya et al. [11] found that, with increasing B_4C ratio in aluminum (Al)-based composites, the hardness and wear resistance of B_4C/Al composites increased, and the Al-16% B_4C composites had the highest hardness and wear resistance. Moreover, Joshi et al. [12] introduced B_4C particles into a magnesium (Mg) alloy matrix, and found that the wear properties and hardness of B_4C/Mg composites were largely improved. Additionally, Hynes et al. [15] found that the mechanical properties of the AA6061 matrix composites were enhanced by adding B_4C reinforcement, and the wear resistance was also superior. At the same time, Aherwar et al. [16] studied the impact of B_4C and porcelain particulates on aluminum (Al) matrix composite properties. They found that both the mechanical and tribological properties were improved, and the wear properties of the Al matrix composites containing 4 wt.% B_4C and 12 wt.% porcelain particulates were the best.

The $B_4C + Me \rightarrow Me_xB_y + C$ graphite reaction occurs between boron carbide and most metals, but copper is one of the few metals that do not have such a reaction. If a new material can be composed of hard B_4C and Cu with good plasticity, it is expected to have high wear resistance and be applied to wear-resisting products, for example, automobile brake clutches. However, so far, there are only a few studies on the impact of B_4C on Cu matrix composites. Moreover, the research is relatively scattered, from different angles, and a lack of systematicness. For example, Prajapati1 et al. [17] fabricated Cu–B_4C composites by cold powder compaction, followed by conventional sintering at 900 °C for 1 h under argon atmosphere, and studied the effect of B_4C content (lower than 15 wt.%) on microstructure, mechanical properties, and electrical conductivity, but the effect of B_4C on the wear-resisting property of the B_4C/Cu composite was not involved. Balalan et al. [18] studied the effect of B_4C on the microstructure and properties of Cu matrix composites that were prepared by hot pressing sintering, but the mass fraction of B_4C was limited to 1.5~6%. Qin et al. [19] prepared Cu-based friction materials with different B_4C mass fractions (3%, 6%, 9%, and 12%) by high-energy ball milling and vacuum sintering, and studied the friction and wear properties of the pair of B_4C/Cu and T10 steel. However, the composite materials also included titanium (Ti), iron (Fe), graphite, rare earth lanthanum, SiC, and other components, which might influence the evaluation of the role of B_4C. Bai et al. [20] prepared B_4C/Cu composites with B_4C volume fractions of 40%–70% by copper plating on B_4C particles and spark plasma sintering, but the main research of the work was the effect of the B_4C surface copper plating process on the thermal conductivity of B_4C/Cu composites.

It is reasonable to infer, from the above analysis, that it is very necessary to further research the impact of B_4C on Cu matrix composites, so as to provide some useful information to extend the project application of B_4C/Cu composites. In this work, B_4C particles were introduced into the Cu matrix to form B_4C/Cu composites by vacuum spark plasma sintering, and the influences of B_4C content (0~20 wt.%) on the microstructures, hardness, density, conductivity, and wear resistance of Cu matrix composites, were systematically studied.

2. Experimental Procedures

2.1. Material Preparing

Raw materials (B_4C powder and Cu powder) were commercially purchased from Nangong Xindun Alloy Welding Material Spraying Co., Ltd., Xingtai, China. The average particle sizes of B_4C powder and Cu powder are 2.5 μm and 2 μm, respectively. The specimen numbers of the B_4C/Cu composites and their corresponding components (wt.%) are presented in Table 1.

Table 1. The specimen numbers of the B_4C/Cu composites and their corresponding components (wt.%).

	BCu0	**BCu5**	**BCu10**	**BCu15**	**BCu20**
Cu	100	95	90	85	80
B_4C	0	5	10	15	20

According to the predesigned composition, an electronic balance was used to weigh powders for five different compositions. Then, each powder mix was ball-milled in a bottle. In the preparation process of the B_4C/Cu composites, we used a laboratory small horizontal mixer to mix the raw materials, and the volume of the cylinder was 10 L. Due to the small amount of powder used in this study, we put it into a 500 mL plastic wide-mouth bottle with dispersant and grinding balls, tightened the bottle lid and fixed it in the barrel of the mixer for mixing. The diameter of the bottle was 80 mm, and the rotation speed was set as 105 r/min. The milling media were absolute ethyl alcohol and aluminum oxide (Al_2O_3) balls. The mixing time was 24 h. After mixing, the absolute ethyl alcohol was thoroughly dried away from the mixture in a vacuum drying oven, and the drying temperature was set as 50 °C. When the composite powder was ready, the powder was placed into a graphite mold and vacuum sintered by using a spark plasma sintering furnace (model: SPS-20T-10). The sintering pressure was 30 MPa, the sinter temperature was 980 °C, and the heat preservation and pressure holding time was 10 min. A B_4C/Cu composite sintering process diagram is shown in Figure 1.

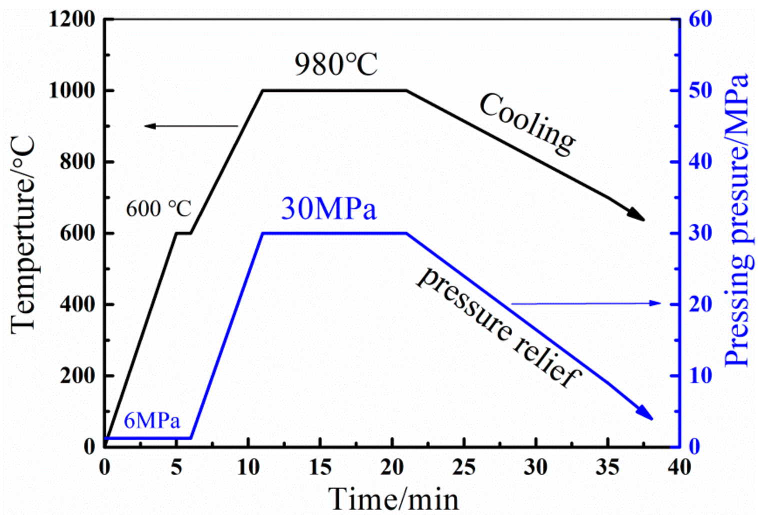

Figure 1. A B_4C/Cu composite sintering process diagram.

The density of sintered B_4C/Cu composites was determined by the Aquimid drainage method. The hardness of sintered B_4C/Cu composites was tested using a digital display Brinell hardness tester (model: 320HBS-3000, Laizhou Huaxing Test Instrument Co., Ltd., Laizhou, China). The electrical conductivity was tested by a digital eddy current metal conductometer (model: Sigma2008B1, Xiamen Tianyan Instrument Co., Ltd., Xiamen, China). Five to ten measurements were made for each performance, and the average value was taken as the final value.

2.2. Wear Resistance Test

An ML-100-type abrasive wear tester was used to test the wear resistance of the sintered B_4C/Cu composite. The schematic diagram of the machine is shown in Figure 2. In the testing process, sintered B_4C/Cu composites served as pin samples to slide against 400# SiC abrasive papers at room temperature. In the wear tester, a B_4C/Cu composite pin specimen that was prefixed in a pin holder was pressed down to contact a 400# SiC abrasive paper that was firmly attached to a holder. The size of the B_4C/Cu composite pin specimens was 5 mm in diameter and 12.5 mm high. One end of the B_4C/Cu composite pin was first ground to a 5-mm-diameter hemisphere surface by a grinding wheel and then polished. The surface roughness (Ra) was less than 1 μm. Before sliding, pins were immersed in acetone, and after 15 min of ultrasonic irrigation, they were thoroughly vacuum dried. The sliding time was 10 min under a load of 10 N in a humidity (50% relative humidity (RH)) and temperature (25 °C) environment.

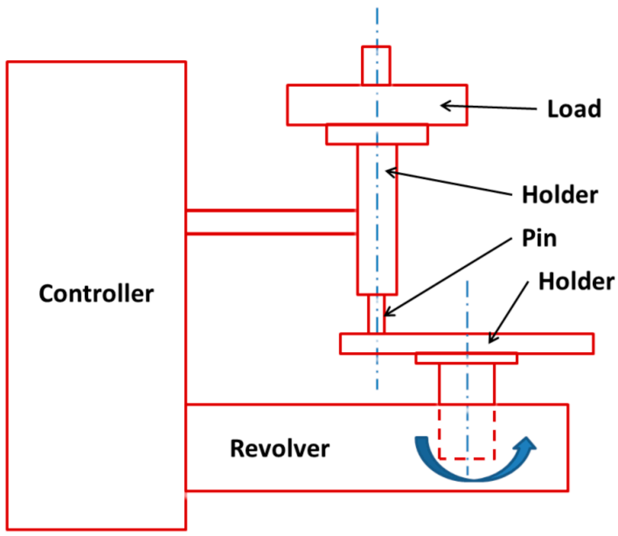

Figure 2. The schematic diagram of the ML-100 type abrasive wear tester.

A laser scanning profilometer (model: VK-9710K, Keenes Ltd., Osaka, Japan) was used to evaluate the wear volume loss of pin specimens. Two orthogonal diameter lengths on the pin worn surface were first measure and then averaged, and the pin wear volume loss was calculated according to the average length of the orthogonal diameters and the initial tip radius. To make a rigorous conclusion, three repeated wear tests were carried out under identical experimental conditions, and the average value was taken as the final value of pin wear volume loss.

Scanning electron microscopy (SEM, TESCAN CHINA, Ltd., Shanghai, China), energy spectrum analysis (EDS, TESCAN CHINA, Ltd., Shanghai, China) and electron probe microanalysis (EPMA, JEOL Ltd., Akishima, Japan) were used to observe and analyze the microstructure and worn surface topographies.

3. Results and Discussion

3.1. Microstructures

Figure 3 presents the B_4C/Cu composite powder morphologies with different amounts of B_4C. As observed in Figure 3a, pure copper powder agglomerates obviously, and extends outward in a dendritic form with poor dispersion. After adding B_4C particles, the B_4C particles would interact with copper powder aggregates during ball milling, to inlay and cut the copper powder aggregates. We can observe, from Figure 3b, that when the B_4C content is 5 wt.%, the dispersibility of the composite powder has shown some improvement. With increasing B_4C content, the dispersibility of the composite powders of Cu-10 wt.%

B_4C (see Figure 3c), Cu-15 wt.% B_4C (see Figure 3d), and Cu-20 wt.% B_4C (see Figure 3e), becomes better and better.

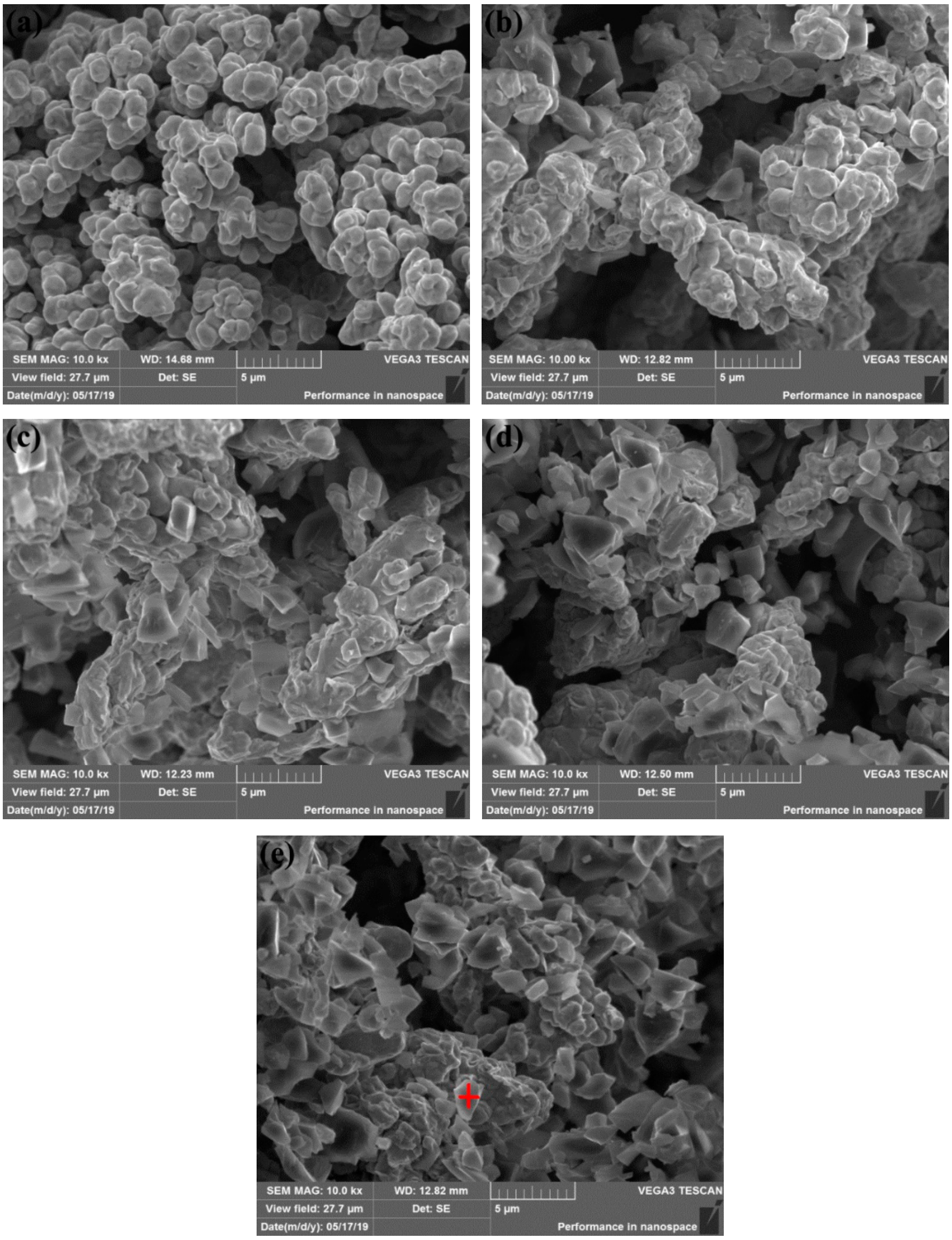

Figure 3. The B_4C/Cu composite powder morphologies with different amounts of B_4C: (**a**) Cu; (**b**) Cu-5 wt.% B_4C; (**c**) Cu-10 wt.% B_4C; (**d**) Cu-15 wt.% B_4C; (**e**) Cu-20 wt.% B_4C.

EPMA analysis was carried out for the small angular and irregular black particles (cross mark in Figure 3e), and the result is shown in Table 2. The B atom percent content is approximately 81%, and the C atom percent content is approximately 18%. The B-to-C atomic ratio is approximately 4:1, so the black particle is in the B_4C phase.

Table 2. EPMA analysis result of the Cu-20 wt.% B_4C powder (cross mark in Figure 2e).

Element	B	C
Content, at.%	80.8	18.2

Figure 4 presents the morphologies of the B_4C/Cu composites under different B_4C contents. The black particles in the morphologies are B_4C particles. To make sure of that, three points (A–C) in the Cu-10 wt.%B_4C composite microstructure were qualitatively analyzed, by using EDS, and the results are shown in Figure 5. A conclusion can be drawn from Figure 5 that the black particles are B_4C particles. As observed in Figure 4, the distribution of B_4C particles is roughly uniform. However, when the content of the B_4C particles was over 15 wt.%, aggregation of B_4C particles occurred.

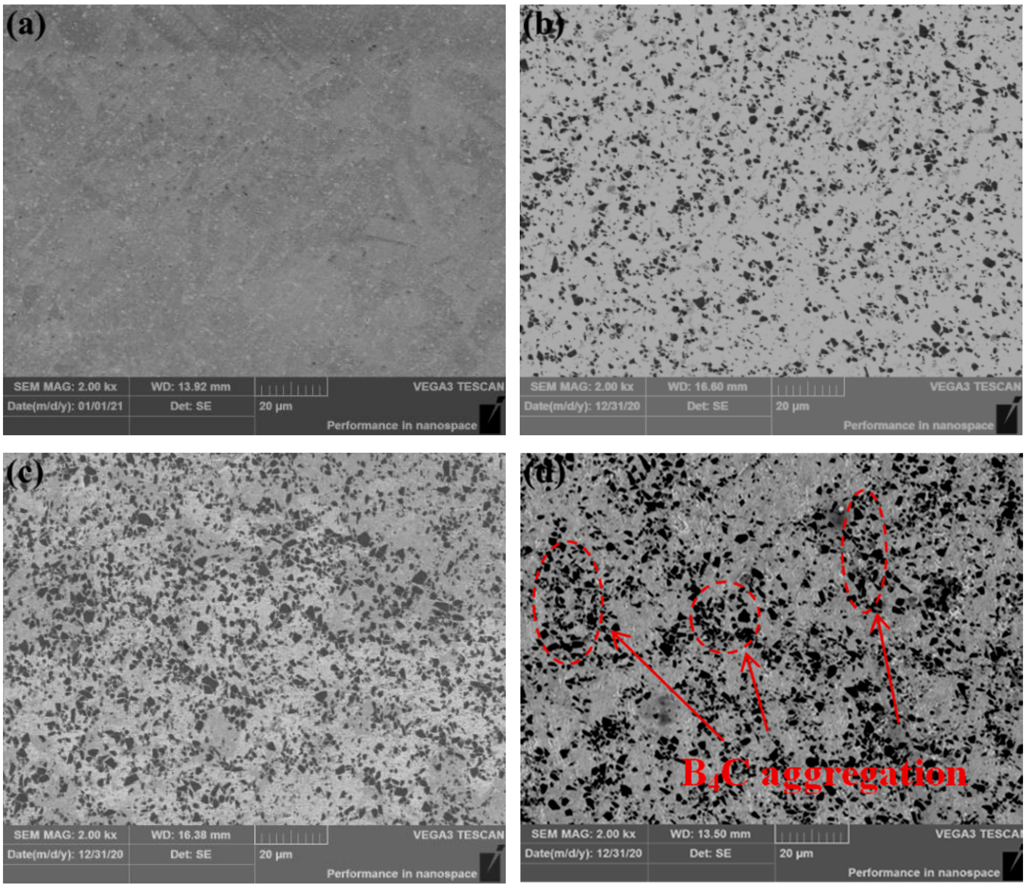

Figure 4. Morphologies of B_4C/Cu composites under different B_4C contents: (**a**) Cu; (**b**) Cu-5 wt.% B_4C; (**c**) Cu-15 wt.% B_4C; (**d**) Cu-20 wt.% B_4C.

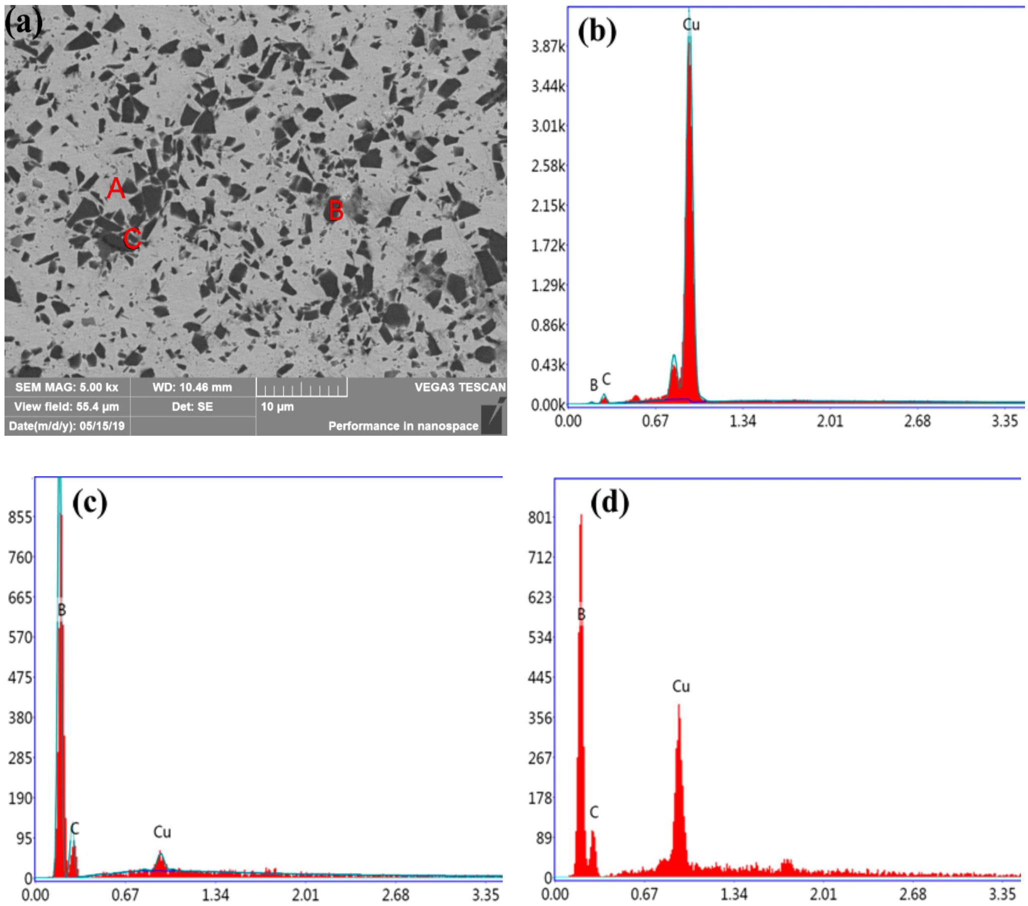

Figure 5. The EDS analysis results of Cu-10 wt.%B_4C composite: (**a**) the microstructure of Cu-10 wt.%B_4C composite; (**b**) EDS analysis of point A; (**c**) EDS analysis of point B; (**d**) EDS analysis of point C.

3.2. Properties of Density, Hardness, and Conductivity

Figure 6 shows the density, hardness, and conductivity of B_4C/Cu composites with different amounts of B_4C. As observed in Figure 6a, the density of pure Cu is 99.1%, and with the increase in the content of B_4C particles, the relative density of the B_4C/Cu composite gradually decreases. The variation trend of the density of B_4C/Cu composites, with the increase in the B_4C content, is consistent with the literature [18]. When the content of B_4C is 20 wt.%, the relative density decreases to 92.3%. There is a significant difference between pure Cu and B_4C. For example, the density of pure Cu is approximately 8.9 g/cm^3, but the density of B_4C is only 2.52 g/cm^3. The hardness of pure Cu is approximately 50 HV, but the hardness of B_4C can reach 55 GPa (approximately 5610 HV). The performance difference may affect the material preparation process, especially the densification of the material. The internal friction between the powders increases with increasing B_4C content, so the resistance to densification increases, resulting in a decrease in the relative density.

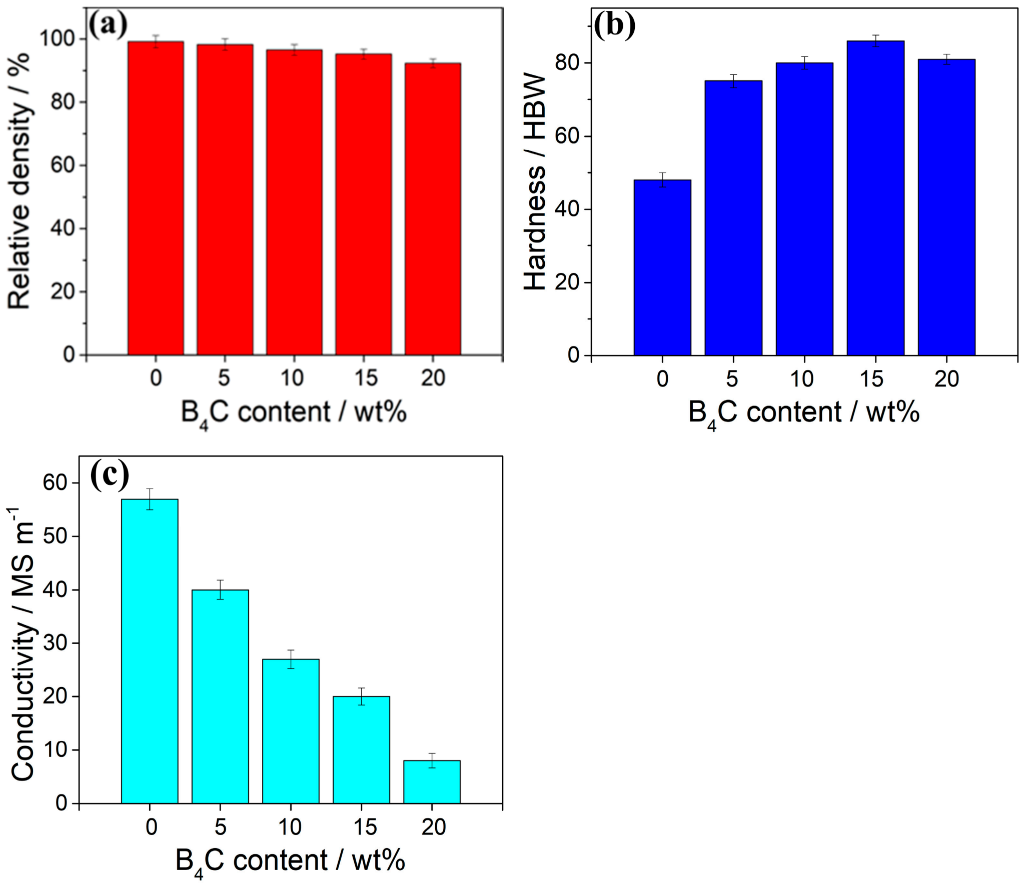

Figure 6. The relative density, hardness and conductivity of B_4C/Cu composites with different amounts of B_4C: (**a**) relative density; (**b**) hardness; (**c**) conductivity.

As observed in Figure 6b, the B_4C/Cu composite hardness first increases and then decreases. The hardness of pure Cu is 48 HBW, but due to the extraordinary hardness of B_4C, when only 5 wt.% is added into the soft Cu matrix, during indentation, B_4C produces resistance to the motion of dislocations, and the hardness of the B_4C/Cu composite increases considerably, from 48 to 75 HBW. In addition, the large differences in the thermal expansion coefficients of copper ($17 \times 10^6/°C$) and B_4C ($5 \times 10^6/°C$) would cause a great thermal expansion mismatch in the sintering process, resulting in the occurrence of a significant amount of dislocation, which is also conducive to an increase in hardness [17]. When the content of B_4C is 15 wt.%, the hardness of the B_4C/Cu composites reaches 86 HBW, which is the highest value. The hardness of the Cu-15 wt.% B_4C composite was 79.2% higher than that of pure Cu. However, when the B_4C amount increases to 20 wt.%, the hardness decreases to 81 HBW. As observed in Figure 6a, the relative density of the Cu-20 wt.% B_4C composite is lower than that of other contents. The voids or pores in the sintered microstructure of the Cu-20 wt.% B_4C composite (see Figure 7) were more, which would weaken the metallic connection in the material, resulting in the reduction in hardness.

The conductivity test results shown in Figure 6c, suggest that pure copper has the best conductivity, at 57 mega Siemens per meter (MS/m). However, the conductivity of the B_4C/Cu composites decreases much more quickly with increasing B_4C content, especially between 0 and 10 wt.% B_4C, and 15 and 20 wt.% B_4C. The main reason is that the conductivity of B_4C is extremely low, the Cu matrix continuity is broken, and B_4C particle networks are formed with increasing B_4C content. Hence, the conductivity of the B_4C/Cu composite largely decreases. The variation trend of the conductivity of B_4C/Cu composites with the increase of B_4C content is consistent with the literature [17].

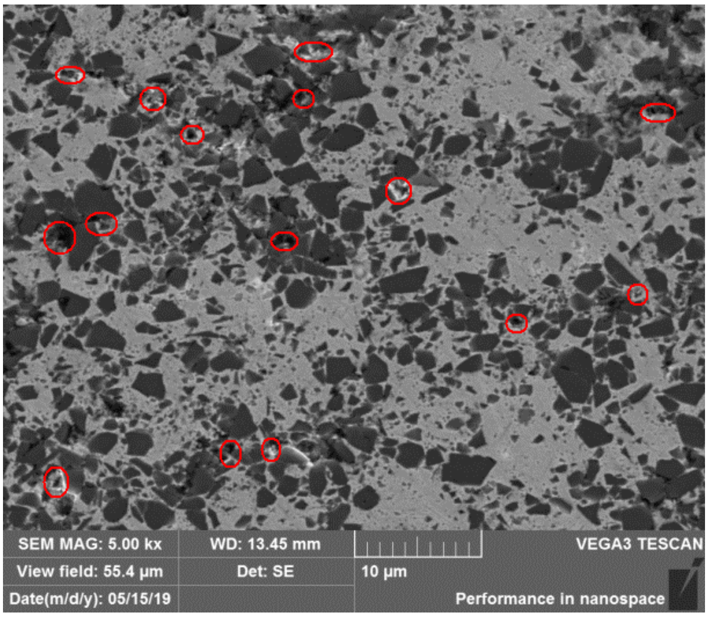

Figure 7. The voids in the sintered microstructure of the Cu-20 wt.% B_4C composite (some voids are marked in red circles).

3.3. Wear-Resisting Property

The wear volume losses of B_4C/Cu composites with different amounts of B_4C are shown in Figure 8, and pure copper has the largest wear volume loss. With increasing B_4C amount, the wear volume loss of the B_4C/Cu composite pin samples decreases first and then increases, so the corresponding wear resistance first increases and then decreases. The volume loss of the Cu-15 wt.% B_4C composite is the lowest, indicating that the Cu-15 wt.% B_4C composite has the best wear resistance.

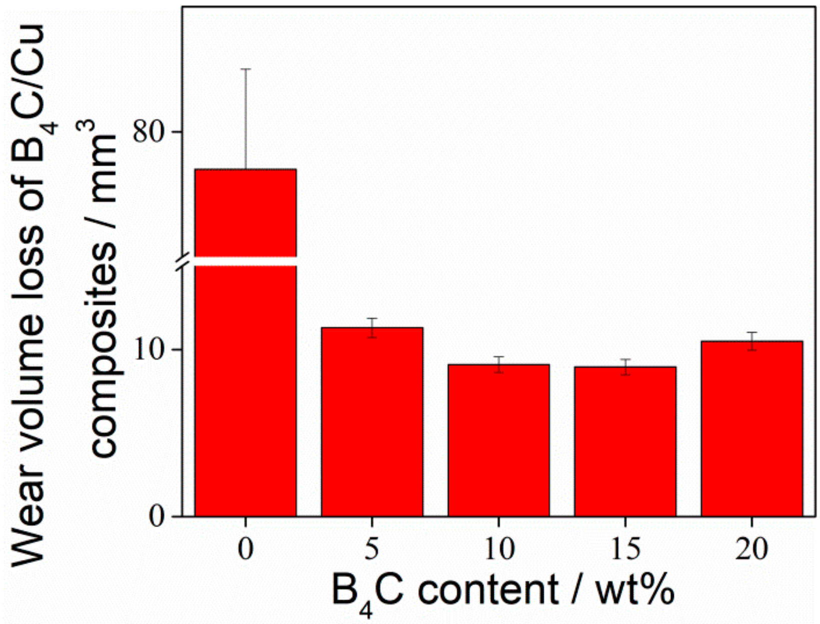

Figure 8. The wear volume loss of the B_4C/Cu composites with different B_4C contents.

To understand the underlying wear mechanisms, the worn morphologies of B_4C/Cu composites under different B_4C contents, after sliding against SiC abrasive papers, were investigated, as shown in Figure 9. As observed in Figure 9a,b, deep and narrow grooves exist on the worn pure Cu surface, indicating severe plastic deformation due to hard granules on the SiC abrasive papers. Additionally, sharp ridges were produced by the plowing mechanism. The worn pure Cu surface EDS analysis shows that the oxygen content is only 2.5 wt.% (see Figure 10), indicating that, during the process of sliding, tribo-oxidation seldom occurred as SiC removed the pure Cu material, and a new surface would be exposed each time hard SiC slid past the pure Cu sample, which caused a high material removal rate of the pure Cu sample.

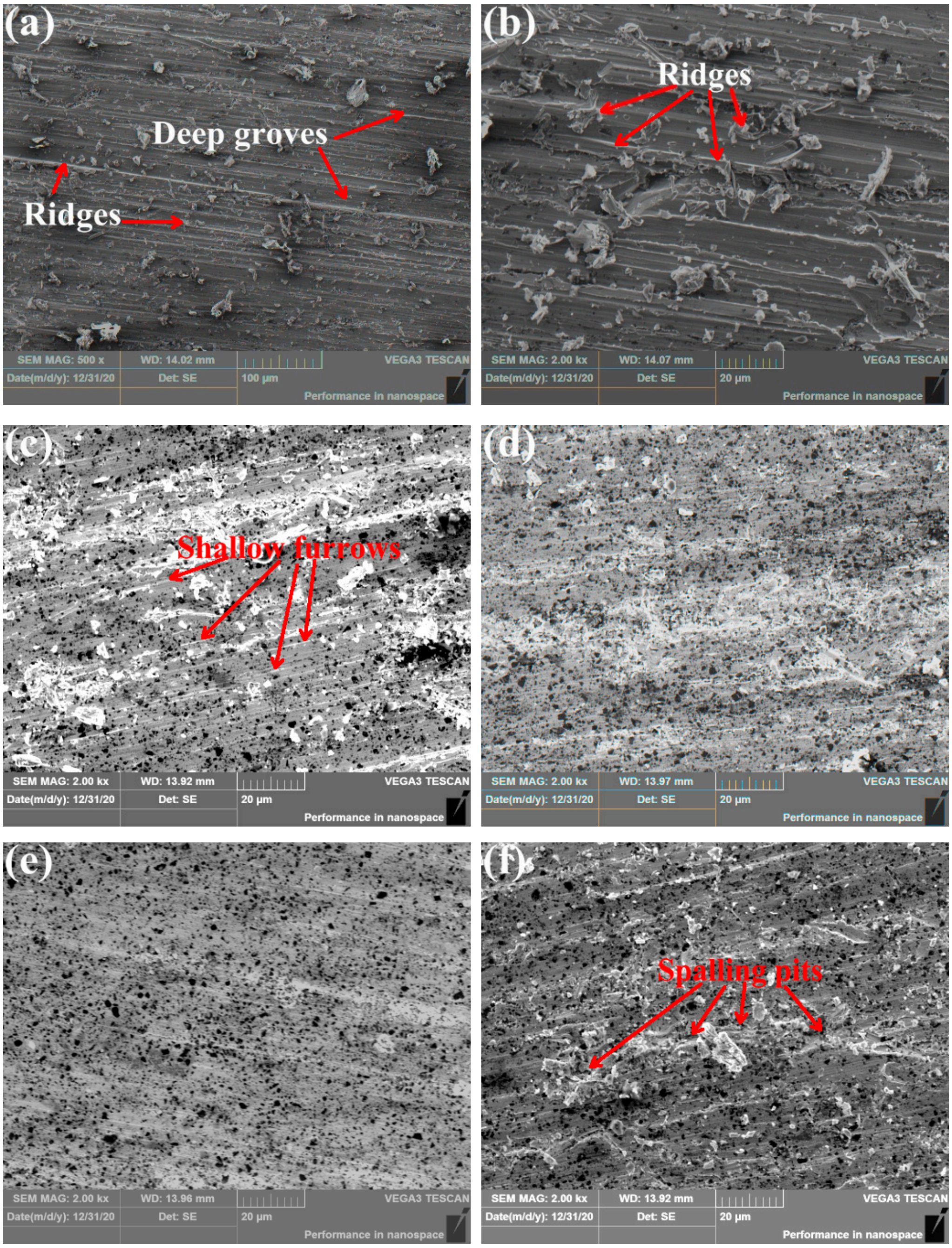

Figure 9. Worn B_4C/Cu composite morphologies with different B_4C contents: (**a**) pure Cu (low magnification); (**b**) pure Cu (high magnification); (**c**) Cu-5 wt.% B_4C; (**d**) Cu-10wt.% B_4C; (**e**) Cu-15 wt.% B_4C; (**f**) Cu-20 wt.% B_4C.

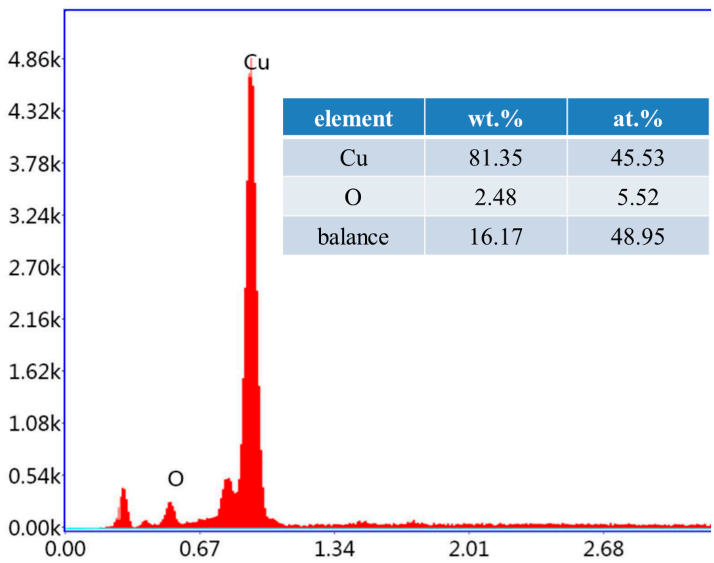

Figure 10. EDS analysis result of the worn pure Cu surface.

As observed in Figure 9c–e, compared with the worn pure Cu morphology, when the B_4C amount is lower than 15 wt.%, the furrows on the worn surfaces of the B_4C/Cu composite pin samples become shallow, and the ridge amount that is formed by plastic deformation decreases with increasing B_4C content. The reason for this is easy to understand. Cu deformation should be restricted by B_4C particles during the sliding process, resulting in the improvement of the wear-resisting property of the B_4C/Cu composite. In particular, ridge formation cannot be found on the worn Cu-15 wt.% B_4C composite surface (see Figure 9e), which represents the enhancement in wear resistance.

When the B_4C content was higher, B_4C particles in the composite easily aggregated (see Figure 4d). In the wear process, these aggregated B_4C particles easily flake off (see Figure 9f), due to the lack of copper phase binding. On the one hand, the flayed B_4C particles between the pin sample and the abrasive paper acted as abrasives, reducing the wear resistance of the composite material. On the other hand, the spalling of B_4C reduces the protective effect on the Cu matrix, and increases the contact area between the Cu matrix and the microconvex peak, which aggravates the wear of the composite material. However, when the B_4C content is 20 wt.%, the impaired sites increase (see Figure 9f). B_4C particles are loosened during the wear process, with the agglomeration of B_4C. As shown in Figure 9f, the entire worn surface of the Cu-20 wt.% B_4C composite shows severe damage. During sliding against the hard SiC abrasives on the abrasive papers and loosened hard B_4C-reinforced particles, spalling phenomena of the Cu matrix occur, which would exhibit more wear loss.

4. Conclusions

In this paper, B_4C/Cu composites with different B_4C contents were obtained by mechanical mixing and discharge plasma sintering methods. The influences of B_4C content on the microstructures, hardness, density, electrical conductivity, and wear resistance of the B_4C/Cu composites, have been studied. Conclusions can be drawn as follows:

(1) The B_4C/Cu composite microstructure analysis shows that, in the Cu matrix, B_4C ceramics are well distributed. However, when the B_4C content is over 15 wt.%, aggregation of the B_4C particles occurs;

(2) Both the relative density and conductivity of the B_4C/Cu composites gradually decrease as the B_4C content increases;

(3) The hardness of the B_4C/Cu composites first increase and then decrease. When the content of B_4C was 15 wt.%, the hardness of the B_4C/Cu composites reached the highest value, 86 HBW, which was 79.2% higher than that of pure Cu. However, when

the B_4C amount increases to 20 wt.%, the hardness decreases, due to the metallic connection being weakened in the material;

(4) The Cu-15 wt.% B_4C composite has the lowest volume loss, indicating that it has the best wear resistance. Analyses of worn B_4C/Cu composite surfaces suggest that deep and narrow grooves, as well as sharp ridges, appear on the worn pure Cu surface, but on the worn Cu-15 wt.% B_4C composite surface, the furrows become shallow and few. In particular, ridge formation cannot be found on the worn Cu-15 wt.% B_4C composite surface, which represents the enhancement in wear resistance.

Based on the above research results and analysis, we can see that B_4C particles have important effects on the microstructures and properties. Some properties, such as hardness and wear resistance, can be improve effectively, but the conductivity performance deteriorates significantly, indicating that B_4C/Cu composites are more suitable to be used in uncharged wear parts. In this work, the wear resistance of the B_4C/Cu composites was evaluated by an ML-100-type abrasive wear tester. However, this testing machine cannot obtain the friction properties (friction coefficient) of the material. To expand the application range of B_4C/Cu composites, in the next step of our work, we will use another friction and wear tester, to further evaluate the friction and wear properties of the B_4C/Cu composites sliding against different metal or ceramic couples under different conditions.

Author Contributions: Conceptualization, D.S. and X.L.; methodology, X.L.; software, Q.Y.; formal analysis, X.L.; investigation, X.L.; writing—original draft preparation, X.L.; writing—review and editing, D.S.; X.L. and Q.Y. All authors have read and agreed to the published version of the manuscript.

Funding: This research was funded by the Scientific and Technological Research Project of Henan province, grant number 212102210453, and the Doctoral Scientific Research Start-up Foundation of Henan University of Science & Technology (Grant No. 13480001 and 13480045).

Institutional Review Board Statement: Not applicable.

Informed Consent Statement: Not applicable.

Data Availability Statement: Not applicable.

Acknowledgments: We wish to take this opportunity to thank the support of the Provincial and Ministerial Collaborative Innovation Center for New Non-ferrous Metal Materials and Advanced Processing Technology.

Conflicts of Interest: The authors declare no conflict of interest. The funders had no role in the design of the study; in the collection, analyses, or interpretation of data; in the writing of the manuscript, or in the decision to publish the results.

References

1. Shaik, M.A.; Golla, B.R. Two body abrasion wear behaviour of Cu-ZrB_2 composites against SiC emery paper. *Wear* **2020**, *450*, 450–451. [CrossRef]
2. Guiderdoni, C.; Estournès, C.; Peigney, A.; Weibel, A.; Turq, V.; Laurent, C. The preparation of double-walled carbon nanotube/Cu composites by spark plasma sintering, and their hardness and friction properties. *Carbon* **2011**, *49*, 4535–4543. [CrossRef]
3. Rabinarayan, S.; Kumar, O.R. Study of Dry-Sliding Wear Behaviour of Cu-SiC_p Metal Matrix Composites. *Mater. Today Proc.* **2020**, *21*, 1255–1259. [CrossRef]
4. Zhao, H.; Feng, Y.; Qian, G.; Huang, X.; Guo, S.; Sun, X. Effect of Ti_3AlC_2 Content on Electrical Friction and Wear Behaviors of Cu-Ti3AlC2 Composites. *Tribol. Lett.* **2019**, *67*, 96. [CrossRef]
5. Li, X.; Wei, S.; Yang, Q.; Gao, Y.; Zhong, Z. Tribological performance of self-matching pairs of B_4C/hBN composite ceramics under different frictional loads. *Ceram. Int.* **2020**, *46*, 996–1001. [CrossRef]
6. Li, X.; Gao, Y.; Yang, Q. Sliding tribological performance of B_4C-hBN composite ceramics against AISI 321 steel under distilled water condition. *Ceram. Int.* **2017**, *43*, 14932–14937. [CrossRef]
7. Li, X.; Gao, Y.; Wei, S.; Yang, Q.; Zhong, Z. Dry sliding tribological properties of self-mated couples of B_4C-hBN ceramic composites. *Ceram. Int.* **2017**, *43*, 162–166. [CrossRef]
8. Li, X.; Gao, Y.; Wei, S.; Yang, Q. Tribological behaviors of B_4C-hBN ceramic composites used as pins or discs coupled with B_4C ceramic under dry sliding condition. *Ceram. Int.* **2017**, *43*, 1578–1583. [CrossRef]

9. Li, X.; Gao, Y.; Song, L.; Yang, Q.; Wei, S.; You, L.; Zhou, Y.; Zhang, G.; Xu, L.; Yang, B. Influences of hBN content and test mode on dry sliding tribological characteristics of B4C-hBN ceramics against bearing steel. *Ceram. Int.* **2018**, *44*, 6443–6450. [CrossRef]
10. Lyu, Y.; Sun, Y.; Jing, F. On the microstructure and wear resistance of Fe-based composite coatings processed by plasma cladding with B_4C injection. *Ceram. Int.* **2015**, *41*, 10934–10939. [CrossRef]
11. Celik, Y.H.; Kilickap, E. Hardness and Wear Behaviours of Al Matrix Composites and Hybrid Composites Reinforced with B4C and SiC. *Powder Metall. Met. Ceram.* **2019**, *57*, 613–622. [CrossRef]
12. Joshi, S.; Yuvaraj, N.; Singh, R.C.; Chaudhary, R. Microstructural and Wear Investigations of the Mg/B_4C Surface Composite Prepared Through Friction Stir Processing. *Trans. Indian Inst. Met.* **2020**, *73*, 3007–3018. [CrossRef]
13. Pandey, S.; Shrivastava, P.K. Vibration-assisted electrical arc machining of 10% B_4C/Al metal matrix composite. *Proc. Inst. Mech. Eng. Part C J. Mech. Eng. Sci.* **2019**, *234*, 1156–1170. [CrossRef]
14. Namini, A.S.; Delbari, S.A.; Nayebi, B.; Asl, M.S.; Parvizi, S. Effect of B_4C content on sintering behavior, microstructure and mechanical properties of Ti-based composites fabricated via spark plasma sintering. *Mater. Chem. Phys.* **2020**, *251*, 123087.
15. Hynes, N.R.J.; Raja, S.; Tharmaraj, R.; Pruncu, C.I.; Dispinar, D. Mechanical and tribological characteristics of boron carbide reinforcement of AA6061 matrix composite. *J. Braz. Soc. Mech. Sci. Eng.* **2020**, *42*, 155. [CrossRef]
16. Aherwar, A.; Patnaik, A.; Pruncu, C.I. Effect of B_4C and waste porcelain ceramic particulate reinforcements on mechanical and tribological characteristics of high strength AA7075 based hybrid composite. *J. Mater. Res. Technol.* **2020**, *9*, 9882–9894. [CrossRef]
17. Prajapati, P.K.; Chaira, D. Fabrication and Characterization of $Cu–B_4C$ Metal Matrix Composite by Powder Metallurgy: Effect of B_4C on Microstructure, Mechanical Properties and Electrical Conductivity. *Trans. Indian Inst. Met.* **2019**, *72*, 673–684. [CrossRef]
18. Balalan, Z.; Gulan, F. Microstructure and mechanical properties of $Cu-B_4C$ and $CuAl-B_4C$ composites produced by hot pressing. *Rare Met.* **2019**, *38*, 1169–1177. [CrossRef]
19. Qin, Q.; Wang, T.; Hua, J. Effect of B_4C Content on Friction and Wear Properties of Copper-based Powder Metallurgy Friction Materials. *Lubr. Eng.* **2017**, *42*, 77–81.
20. Bai, H. Preparation and Research of Diamond (Boron Carbide)/Metal Composite Encapsulation Material. Ph.D. Thesis, Huazhong University of Science and Technology, Wuhan, China, 2013.